Analysis of the Growth Mechanism of Coprecipitated Spherical and Dense Nickel, Manganese, and Cobalt-Containing Hydroxides in the Presence of Aqueous Ammonia

Andrew van Bommel[†] and J. R. Dahn*[,†,‡]

Department of Chemistry and Department of of Physics and Atmospheric Science, Dalhousie University, Halifax, Nova Scotia, Canada B3H 3J5

Received November 19, 2008. Revised Manuscript Received February 19, 2009

Spherical and dense metal hydroxides were synthesized with a coprecipitation reaction in the presence of aqueous ammonia. The growth of the particles was studied by tracking the tap density and morphology with reaction time. The dependence of pH on the tap density and morphology of the particles synthesized in the coprecipitation reaction was determined for $Ni(OH)_2$, $Ni_{1/2}Mn_{1/2}(OH)_2$, and $Ni_{1/3}Mn_{1/3}Co_{1/3}(OH)_2$ The pH range at which particle growth occurred varied for the different metal hydroxides. Solving the chemical equilibria present in the coprecipitation reaction revealed that the pH range at which spherical particle growth occurred was due to the presence of metal coordinated with ammonia. On the basis of the experiments and analysis presented here, the metal hydroxide particle growth occurs by a dissolution−recrystallization type mechanism during synthesis.

Introduction

Many studies have been carried out on the synthesis of dense, spherical hydroxides by using a coprecipitation reaction in the presence of ammonia. These include the preparation of dense, spherical nickel hydroxide to be used in nickel metal hydride batteries.[1−10] Dense, spherical metal hydroxides have also been made with mixed metals, including nickel, manganese, and cobalt (NMC).[11−19] NMC hydroxides are precursors to lithium-NMC oxides, positive electrode materials for lithium-ion batteries.[20−22]

The typical growth mechanism for the synthesis of dense, spherical hydroxide particles in the presence of ammonia has been presented by several researchers.[3,6,9,16,23] These researchers state that the metal ions from the incoming salt solution first coordinate to the ammonia present in solution, and then are slowly released to the basic solution to yield dense, spherical hydroxide particles. A general scheme of this reaction is given below.

$$M^{2+} + nNH_3 \rightarrow [M(NH_3)_n]^{2+}$$

$$[M(NH_3)_n]^{2+} + 2OH^- \rightarrow M(OH)_2 + nNH_3$$

In the present study, the growth of metal hydroxide particles, including $Ni(OH)_2$, $Ni_{1/2}Mn_{1/2}(OH)_2$, and $Ni_{1/3}Mn_{1/3}Co_{1/3}(OH)_2$, in the presence of ammonia is studied. A new mechanism for dense, spherical hydroxide particle growth is presented.

Experimental Section

Reagents used in this investigation included nickel(II) sulfate hexahydrate (98%, Alfa Aesar), manganese sulfate monohydrate (Alfa Aesar, 98%), cobalt sulfate heptahydrate (Alfa Aesar, 98%), sodium hydroide (Alfa Aesar), and ammonium hydroxide (28.0−30.0%, Sigma-Aldrich). All solutions were prepared with deionized water that was deaerated by boiling for 10 min.

A coprecipitation reactor with a 2 L jacketed reaction vessel equipped with pH and temperature controllers was used in this investigation. Reagents were added using digital peristaltic pumps

* Corresponding author. E-mail: jeff.dahn@dal.ca.
† Department of Chemistry, Dalhousie University.
‡ Department of of Physics and Atmospheric Science, Dalhousie University.

(1) Makimoto, K.; Sekimoto, M.; Fujikake, S.; Ishii, M. European Patent 0649818 A1, 1994.
(2) Konstantinov, K.; Zhong, S.; Wang, C.; Liu, H.; Dou, S. Australian Patent 2002100001 A4, 2002.
(3) Shin, D. Y. U.S. Patent 5 587 139, 1996.
(4) Shin, D. Y. U.S. Patent 5 498 403, 1996.
(5) Ikoma, M.; Akutsu, N.; Enokido, M.; Yoshii, F.; Kaiya, H.; Tsuda, S. U.S. Patent 5 700 596, 1997.
(6) Aladjov, B. U.S. Patent 5 788 943, 1998.
(7) Wakao, S. U.S. Patent 5 861 131, 1999.
(8) Zhaorong, C.; Gongan, L.; Yujuan, Z.; Jianguo, C.; Yunchange, D. *J. Power Sources* **1998**, *74*, 252.
(9) Junichi, I.; Yuri, K.; Tetsushi, M.; Toyoshi, I. U.S. Patent 6 040 007, 2000.
(10) Ovshinsky, S.; Aladjov, B.; Young, R.; Vankatesan, S.; Dhar, S. U.S. Patent 6 086 843, 2000.
(11) Komatsu, K.; Makizoe, S.; Kamada, T.; Ochi, Y.; Okito, T. U.S. Patent 6 132 639, 2000.
(12) Cho, J.; Park, B. *J. Power Sources* **2001**, *92*, 35.
(13) Ito, M.; Usui, T.; Shimakawa, M.; Iida, T. U.S. Patent 2002/0063663 A1, 2002.
(14) Ying, J.; Wan, C.; Jiang, C.; Li, Y. *J. Power Sources* **2001**, *99*, 78.
(15) Ohzuku, T.; Yoshizawa, H.; Nagayama, M. U.S. Patent 2003/0054250 A1, 2003.
(16) Lee, M. H.; Kang, Y. J.; Myung, S. T.; Sun, Y. K. *Electrochim. Acta* **2004**, *50*, 939.
(17) He, P.; Wang, H.; Qi, L.; Osaka, T. *J. Power Sources* **2006**, *160*, 623.
(18) Cho, J.; Kim, G.; Park, Y.; Kim, S. U.S. Patent 6 773 852 B2, 2004.
(19) Sun, J.; Cheng, J.; Wang, C.; Ma, X.; Li, M.; Yuan, L. *Ing. Eng. Chem. Res.* **2006**, *45*, 2146.
(20) Ohzuku, T.; Makimura, Y. *Chem. Lett.* **2001**, 642.
(21) Lu, Z.; MacNeil, D. D.; Dahn, J. R. *Electrochem. Solid-State Lett.* **2001**, *4*, A200–A203.
(22) Paulsen, J. M.; Kiey, L. Y., Ammundsen, B. G. U.S. Patent 5 550 432 B2, 2003.
(23) Cho, J. *Chem. Mater.* **2000**, *12*, 3089.

10.1021/cm803144d CCC: $40.75
Published on Web 03/18/2009

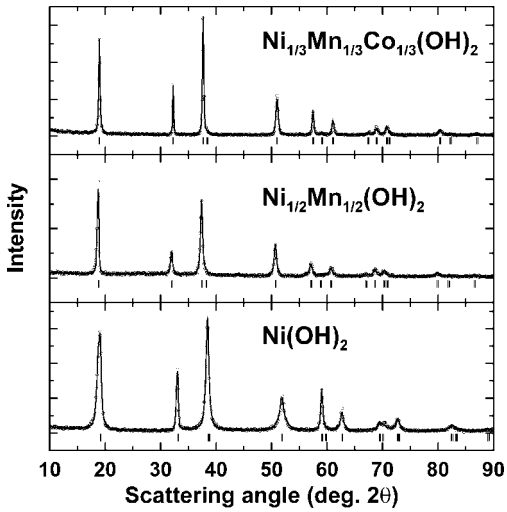

Figure 1. XRD patterns of $Ni(OH)_2$, $Ni_{1/2}Mn_{1/2}(OH)_2$, and $Ni_{1/3}Mn_{1/3}Co_{1/3}(OH)_2$. The solid curve in each panel is the calculated pattern using Rietveld profile analysis and the parameters listed in Table 1.

(Masterflex L/S 07524) and sodium hydroxide addition was automatically controlled by the pH controller and added as required by a peristaltic pump on the reactor. Reaction contents were maintained at a temperature of 60 °C and the contents of the reactor were stirred by an overhead stirrer at 1000 rpm. Nitrogen was bubbled (60 sccm) into the reactor throughout the reaction.

The pH meter and electrode (Mettler-Toledo InLab 424) were calibrated at 60 °C using buffer solutions. The pH values of the buffer solutions were 7.0 at 60 °C (Fisher Scientific) and 11.1 at 60 °C (Fixanal, Riedel-de Haën). When required, the pH electrode was rinsed with dilute HCl to remove deposited hydroxide.

A volume of 1 L of a 1 M NH_3(aq) solution made in deaerated water was heated to 60 °C. The reaction proceeded with the addition of 10.0 M NH_3(aq) at 0.005 L/h and 2.0 M MSO_4 (M = Ni, Co, and/or Mn in desired ratios) at 0.035 L/h. A concentration of 5.0 M NaOH was automatically added to the reaction contents to maintain the desired pH. The rate of NaOH solution addition was near the predicted value of 0.02 L/h based on the expected coprecipitation reaction.

The reaction vessel was fitted with an overflow pipe and the reaction contents were pressurized with nitrogen to ensure a constant volume during the reaction. The residence time, given by the total flow rate of the reagents and the reactor volume, was set to be 10 h. After reaction, the solid material was filtered and washed with 3 L of deaerated deionized water in several rinses.

A Siemens D5000 diffractometer equipped with a Cu-target X-ray tube and a diffracted beam monochromator was used to collect powder diffraction patterns of the synthesized materials. A Hitachi S4700 field-emission scanning electron microscope (SEM) was used to image the materials. Tap densities were determined using a VanKel tap density measuring device. A 25 mL graduated cylinder and 1000 taps were used.

Results and Discussion

Figure 1 shows examples of X-ray diffraction (XRD) patterns for $Ni(OH)_2$, $Ni_{1/2}Mn_{1/2}(OH)_2$, and $Ni_{1/3}Mn_{1/3}Co_{1/3}(OH)_2$ as prepared in this study along with calculated patterns using Rietveld profile analysis with the Reitica software.[24] The calculations used space group $P\bar{3}m$ with metal atoms in 1a sites and oxygen atoms in 2d sites. The refined lattice constants and oxygen positional parameters are given in Table 1. Figure 1 shows that the Bragg peak positions match those of the calculated hydroxide pattern and that oxidation to oxyhydroxide has not yet occurred.

Table 1. Hexagonal Lattice Constants and *z*-Position of the Oxygen Atom Calculated for $Ni(OH)_2$, $Ni_{1/2}Mn_{1/2}(OH)_2$, and $Ni_{1/3}Mn_{1/3}Co_{1/3}(OH)_2$

material	z_O	a (Å)	c (Å)
$Ni(OH)_2$	0.239	3.128	4.643
$Ni_{1/2}Mn_{1/2}(OH)_2$	0.252	3.224	4.705
$Ni_{1/3}Mn_{1/3}Co_{1/3}(OH)_2$	0.247	3.207	4.688

We used the anisotropic broadening capability of the Reitica software in order to simulate the broad and narrow peaks most evident in the $Ni(OH)_2$ sample. The half-width, H, of the peaks is represented by

$$H_k = ((U + U_{anis})\tan^2\theta + V\tan\theta + W)^{1/2} \quad (1)$$

where U_{anis} is given by

$$U_{anis} = U_a\cos 2\phi \quad (2)$$

and ϕ is the angle between the (001) reciprocal lattice vector and the (hkl) reciprocal lattice vector, and U, U_a, V, and W are adjustable parameters. This expression preferentially broadens the (00L) peaks relative to the (hk0) peaks. Peaks with mixed in-plane and out-of-plane character are broadened to an intermediate extent. Although this does not capture the physics of stacking faults properly, it is sufficient to allow an acceptable fitting of the X-ray diffraction profile.

It is believed that the particles have homogeneous cation content: the lattice constants of the hydroxides depend strongly on Ni, Mn, and Co content,[25] whereas the X-ray patterns show sharp (especially (100) and (110)) Bragg peaks suggesting homogeneous materials.

Nickel hydroxide was prepared in the presence of aqueous ammonia. Samples of the synthesized nickel hydroxide were extracted throughout the reaction. Figure 2 shows the dependence of the tap density of the sample on the reaction time. The tap density of the nickel hydroxide follows an asymptotic curve, increasing to 2.1 g cm^{-3} after 20 h.

Figure 3 shows the dependence of particle morphology on the reaction time. The nickel hydroxide secondary particle grows during the reaction. As well, there are smoother surfaces of the secondary particles at higher reaction times. The increase in tap density with reaction time can be

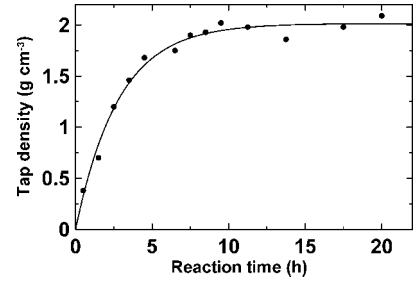

Figure 2. Tap density of $Ni(OH)_2$ as a function of reaction time (pH 11.0).

(24) Hunter, B. A. *Rietica for Windows*, version 1.7.7; Australian Nuclear Science and Technology Organisation: Sydney, Australia, 1997.

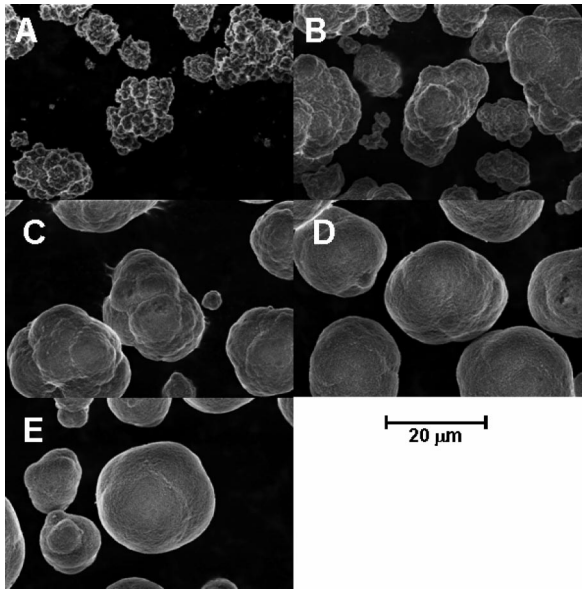

Figure 3. SEM images of $Ni(OH)_2$ a function of reaction time for (A) $t = 2$ h; (B) $t = 5$ h; (C) $t = 10$ h; (D) $t = 15$ h; and (E) $t = 20$ h (pH 11.0).

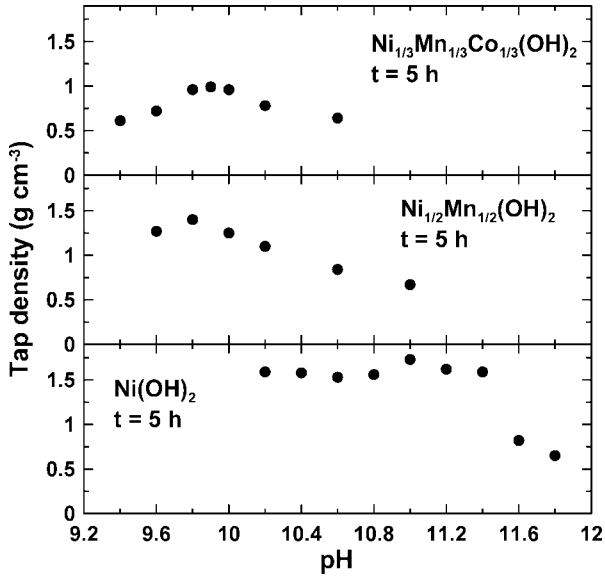

Figure 4. Dependence of tap density on pH of $Ni(OH)_2$, $Ni_{1/2}Mn_{1/2}(OH)_2$, and $Ni_{1/3}Mn_{1/3}Co_{1/3}(OH)_2$ for $t = 5$ h.

attributed to (1) the increase in tap density of the secondary particle evident by the smooth surfaces at higher reaction times; (2) thickening of the plate-like primary particles, decreasing the porosity of the secondary particles and (3) the decrease in irregular-shaped particles, which would lead to effects such as bridge formation, lowering the overall tap density of the sample.

Figure 4 shows the effect of pH on the tap density of $Ni(OH)_2$, $Ni_{1/2}Mn_{1/2}(OH)_2$, and $N_{i1/3}Mn_{1/3}Co_{1/3}(OH)_2$. A relatively short reaction time of 5 h was used, which gave relatively low tap densities for the hydroxide samples. In the case of $Ni(OH)_2$, high tap density materials can be made at pH values of 11.4 or less. At pH values greater than 11.4, there is a large decrease in tap density, which indicates that dense, spherical particles cannot be synthesized at these pH values. For $Ni_{1/2}Mn_{1/2}(OH)_2$ and $Ni_{1/3}Mn_{1/3}Co_{1/3}(OH)_2$, dense, spherical particle growth occurs at pH values of less than 10.2. Manganese and cobalt have an effect on the pH value that is required for dense, spherical particle growth in the presence of aqueous ammonia.

Figure 5 shows the SEM images of $Ni(OH)_2$ prepared at various pH-values. All morphologies at pH values of 11.4 and lower indicated dense, spherical particle growth. The $Ni(OH)_2$ sample prepared at a pH value of 11.8 shows that spherical particle growth is not taking place.

The dependence of the required pH for hydroxide particle growth on the metal(s) was studied by investigating the chemical equilibria present during the reaction. The equilibrium constants used were the equilibrium constants for coordination of ammonia to the metal ions, the base dissociation constant of aqueous ammonia, the solubility product of the metal hydroxide, and the water dissociation constant.[26] Table 2 shows the relevant equilibria and the mass balances for $Ni(OH)_2$, $Mn(OH)_2$, and $Co(OH)_2$. For clarity, the coordinating water molecules (as in$[M(H_2O)_6]^{2+}$) are not indicated. These equilibria were solved for various pH-values with the total metal concentration ($C_{M^{2+}}$) and total ammonia concentration (C_{NH_3}) as 2 and 1 M, respectively for various pH values. It should be noted that the equilibrium constants were all for 25 °C, whereas the reaction temperature in the experimental study was 60 °C.

The concentrations of all relevant species were determined as a function of pH value. Figure 6 shows the effect of pH on the concentration of the sum of all metal-ammonia complexes ($[M(NH_3)_n]^{2+}$) for nickel, manganese, and cobalt. Nickel shows coordination with ammonia at pH 4−12, whereas manganese and cobalt coordinate with ammonia in a smaller pH range: pH 6−10. This is in agreement with the experimental data: Figure 4 shows that manganese and cobalt containing hydroxides form materials with higher tap densities at lower pH-values than the pH values needed to synthesize spherical and dense $Ni(OH)_2$. Considering that spherical particle growth only occurs with interaction of metal and ammonia, manganese and cobalt-containing hydroxides require a lower pH value than nickel-containing hydroxides for ammonia coordination, and therefore, for the conditions for spherical particle growth.

In view of the growth of hydroxide particles with time, the dependence of particle morphology on pH, and analysis of the relevant equilibria present in the coprecipitation reaction, the authors suggest an alternate growth mechanism for spherical hydroxide growth in the presence of aqueous ammonia. Rather than a metal ion first coordinating with ammonia and then being slowly released to the basic solution, the growth of hydroxide particles is due to the equilibrium between metal hydroxide particles and aqueous ammonia solution. In this mechanism, the metal hydroxide has an effective increased solubility in the presence of aqueous ammonia. This is shown in the equilibrium below.

(25) Wyckoff, R. *Crystal Structures*; Interscience Publishers: New York, 1982.
(26) Sillen, L. G. *Stability Constants of Metal-Ion Complexes*; Chemical Society: London, 1964.

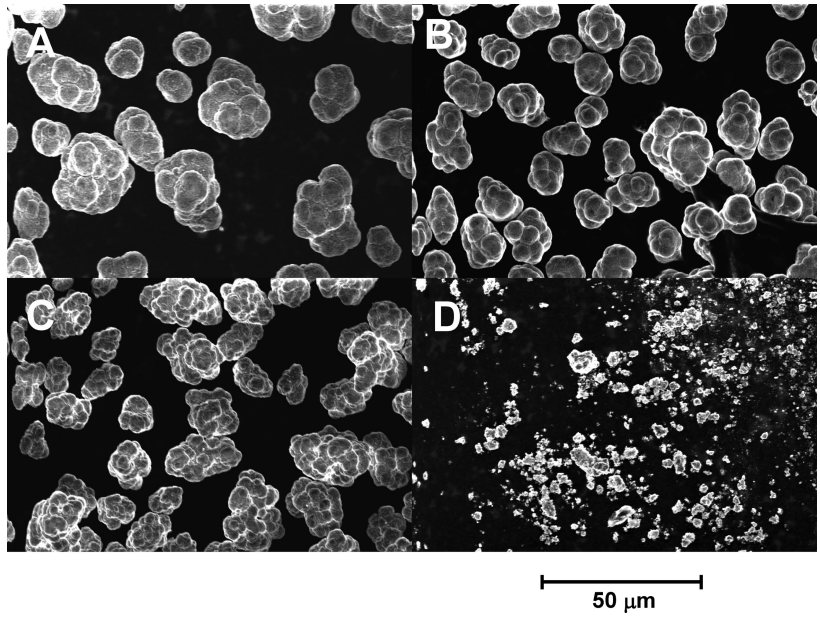

Figure 5. SEM images of $Ni(OH)_2$ synthesized for $t = 5$ h with a pH value of (A) 10.6, (B) 11.0, (C) 11.4, and (D) 11.8.

Table 2. Equilibria and Mass Balances Solved to Determine the Concentration of Species Present in the Reactor at Various pH Values

		log K		
equilibrium reaction	K	Ni	Mn	Co
$M^{2+} + NH_3 \rightleftharpoons [M(NH_3)]^{2+}$	K_1	2.81	1.00	2.10
$M^{2+} + 2NH_3 \rightleftharpoons [M(NH_3)_2]^{2+}$	K_2	5.08	1.54	3.67
$M^{2+} + 3NH_3 \rightleftharpoons [M(NH_3)_3]^{2+}$	K_3	6.85	1.70	4.78
$M^{2+} + 4NH_3 \rightleftharpoons [M(NH_3)_4]^{2+}$	K_4	8.12	1.3	5.53
$M^{2+} + 5NH_3 \rightleftharpoons [M(NH_3)_5]^{2+}$	K_5	8.93		5.75
$M^{2+} + 6NH_3 \rightleftharpoons [M(NH_3)_6]^{2+}$	K_6	9.08		5.14
$NH_3 + H_2O \rightleftharpoons NH_4^+ + OH^-$	K_b	−4.80	−4.80	−4.80
$M(OH)_2 \rightleftharpoons M^{2+} + 2OH^-$	K_{sp}	−15.22	−12.70	−14.89
$H_2O \rightleftharpoons H^+ + OH^-$	K_w	−14	−14	−14

mass balances

$C_{M^{2+}} = [M^{2+}] + [Ni(OH)_2] + [M(NH_3)_2{}^{2+}] + [M(NH_3)_3{}^{2+}] + [M(NH_3)_4{}^{2+}] + [M(NH_3)_5{}^{2+}] + [M(NH_3)_6{}^{2+}]$

$C_{NH_3} = [NH_3] + [M(NH_3)^{2+}] + 2[M(NH_3)_2{}^{2+}] + 3[M(NH_3)_3{}^{2+}] + 4[M(NH_3)_4{}^{2+}] + 5[M(NH_3)_5{}^{2+}] + 6\,[M(NH_3)_6{}^{2+}]$

$$M(OH)_2 + nNH_3 \rightleftharpoons [M(NH_3)_n]^{2+} + 2OH^-$$

The strength of dissolution of metal hydroxide has been shown to be dependent on the pH of the reaction, which varies depending on the metal involved. Spherical hydroxide particle growth in the presence of aqueous ammonia therefore is due to a dissolution−recrystallization mechanism. In such a mechanism, small particles will be consumed in favor of larger particles to minimize surface free energy.

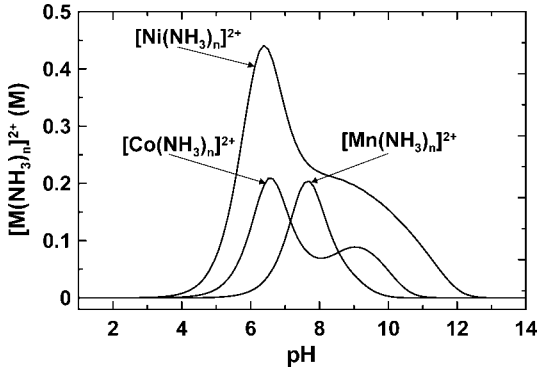

Figure 6. Effect of pH on the concentration of $[Ni(NH_3)_n]^{2+}$, $[Mn(NH_3)_n]^{2+}$, and $[Co(NH_3)_n]^{2+}$. The curve is the sum of the concentrations for complexes with $1 \leq n \leq 6$.

Conclusions

Spherical and dense nickel, manganese, and cobalt-containing hydroxides can be prepared in the presence of aqueous ammonia. The growth of the metal hydroxide occurs throughout the reaction time, which results in higher tap-density material. The conditions for particle growth depend on the pH of the reaction, which varies for different metal hydroxides. The pH values required for spherical hydroxide growth varies since the pH range at which coordination to ammonia occurs is different for nickel, manganese, and cobalt. The spherical particle growth is due to the increase in solubility of the metal hydroxide in the presence of aqueous ammonia. Spherical particle growth in the presence of ammonia takes place by a dissolution−recrystallization mechanism.

The analysis of chemical equilibria present during the coprecipitation reaction can be used as a prediction of the materials obtained. For example, spherical particle growth is unlikely to occur with salts that have metal cations that do not coordinate with ammonia. For the case where the metal does coordinate with ammonia, the pH values at which the concentration of metal−ammonia coordinated complexes can be calculated. If chemical equilibria calculations are carried out at a variety of temperatures and reagent concentrations, this could be a powerful tool in the prediction of the characteristics of the hydroxide material.

Acknowledgment. The authors thank NSERC and 3M Canada for funding this work under the auspices of the industrial chairs program. A.v.B. also thanks Vincent Chevrier for assistance in solving the coupled equations for the chemical equilibria and NSERC for scholarship support. The authors thank Junwei Jiang and Mark Obrovac for numerous useful discussions.

CM803144D